

Thermodynamic modeling of a nuclear energy based integrated system for hydrogen production and liquefaction



Hasan Ozcan^{a,b,*}, Ibrahim Dincer^{b,c}

^a Faculty of Engineering, Karabuk University, 100. Yil Mh, Demir Celik Kampusu, Karabuk, 78050, Turkey

^b Clean Energy Research Laboratory, Faculty of Engineering and Applied Science, University of Ontario Institute of Technology, 2000 Simcoe Street North, Oshawa, Ontario L1H 7K4, Canada

^c Department of Mechanical Engineering, King Fahd University of Petroleum and Minerals, Dhahran 31261, Saudi Arabia

ARTICLE INFO

Article history:

Received 2 February 2016

Received in revised form 7 April 2016

Accepted 8 April 2016

Available online 13 April 2016

Keywords:

Nuclear power plant

Mg–Cl cycle

Hydrogen production

Hydrogen liquefaction

Energy

Exergy

ABSTRACT

A nuclear based integrated system for hydrogen production and liquefaction with a newly developed four-step magnesium–chlorine cycle is proposed. The system uses nuclear energy to supply heat for the Rankine cycle and Mg–Cl cycle, where the power produced by the Rankine cycle is used to run the electrolysis steps of the Mg–Cl cycle and liquefaction cycle compressors. The four-step Mg–Cl cycle is specifically designed to decrease the electrical work consumption of the cycle by capturing HCl in dry form with an additional step to conventional three-step cycle. A performance assessment study is undertaken based on energy and exergy analysis of the subsystems, and total energy and exergy efficiencies of the plant are found to be 18.6%, and 31.35%. The comparisons of the subsystem efficiencies and total exergy destructions show that highest irreversibility ratio belongs to the Mg–Cl cycle by 41%, respectively.

© 2016 Elsevier Ltd. All rights reserved.

1. Introduction

Energy is treated as one of the most crucial matters for society, environment, resources, and even for international relations. Limited energy resources have major effects on mechanisms of decision making. Use of fossil fuels has a dominating effect of all mentioned parameters on human being, specifically for environment. Hydrogen has, so far, been the most promising energy carrier as alternative to fossil fuels as a clean solution, where there are several possible ways to produce it in a more sustainable way. Hydrogen can be produced from both primary and secondary energy sources. Commercially applicable methods generally consist of fuel processing and the required energy is provided from primary energy sources such as coal and CH₄. Although natural gas reforming and coal gasification are commercially available, much research is performed to improve efficiency of existing plants. Biomass based hydrogen production is still under development and not yet commercially available. Hydrogen production from secondary energy resources are exclusively by water electrolysis using electricity. So

far, the highest rate of direct hydrogen production is occupied by steam methane reforming. However, renewable based hydrogen production with several types of methods can be a good candidate to compete with conventional hydrogen production methods (Dincer and Zamfirescu, 2012). Many sustainable hydrogen production technologies have recently been proposed by researchers in the field using conventional and renewable energy resources by providing zero emission plants and their optimization (Georgis et al., 2011; Montazer-Rahmati and Binaee, 2010; Zhu et al., 2016).

Although the renewable energy sources are good candidates to supply energy needs of the communities in a clean and sustainable way, maturity of renewable based energy plants are still an ongoing process and intermittent nature of most renewables can be a limiting factor for continuous energy supply. Thus, nuclear energy is one of the most promising energy supply sources with mature technologies at very large range of capacities (Naterer et al., 2013).

Nuclear energy is converted into thermal energy within a fission reaction, and to mechanical energy with conversion units such as steam Rankine cycle. Nuclear power plant efficiencies vary from 30 to 40% dependent on the technology used, and these plants generate 16% of global electricity demand. Major losses throughout the plant are due to thermal to mechanical energy conversion. It is possible to use the medium to high temperature thermal energy to supply heat for some endothermic reaction steps, and heating processes of thermochemical cycles to produce hydrogen. Nuclear

* Corresponding author at: Faculty of Engineering, Karabuk University, 100. Yil Mh, Demir Celik Kampusu, Karabuk, 78050, Turkey.

E-mail addresses: HasanOzcan@karabuk.edu.tr, hasozc@gmail.com (H. Ozcan), Ibrahim.Dincer@uoit.ca (I. Dincer).

Nomenclature

C_p	Specific heat (kJ/kg°C)
ex	Specific exergy (kJ/kg)
Ex	Exergy rate (kW)
f	Splitting factor
G^0	Gibbs free energy
h	Specific enthalpy (kJ/kg)
\dot{m}	Mass flow rate (kg/s or L/min)
\dot{Q}	Heat transfer rate (kW)
s	Specific entropy (kJ/kg K)
\dot{S}	Entropy rate (kW/T)
R	Universal gas constant (kJ/kmolK)
T_0	Ambient temperature (K or °C)
\dot{W}	Power (kW)

Greek symbols

η	Efficiency
--------	------------

Subscripts

abs	Absorbed
ch	Chemical
cv	Control volume
d	Destruction
en	Energy
ex	Exergy
f	Flow
kin	Kinetic
ph	Physical
pot	Potential
s	Solid
sys	System
tot	Total

Superscripts

Q	Heat
0	Thermomechanical equilibrium
00	Chemical equilibrium

Acronyms

CANDU	Canada Deuterium Uranium
HEX	Heat exchanger
Mg-Cl	Magnesium chlorine
SCWR	Supercritical water reactor
SRC	Steam Rankine cycle

based hydrogen production can be accomplished by several water splitting methods (Ozcan and Dincer, 2014a).

Mg-Cl cycle was initially proposed as a three-step process where no consideration of higher steam requirement for hydrolysis reaction has been made, which leads to aqueous HCl electrolysis (1.8 V) at higher voltage requirements than dry HCl electrolysis (1.4 V). Various configurations of the Mg-Cl cycle are represented in Table 1 (Ozcan and Dincer, 2014a,b, 2015a,b). A newly developed four-step Mg-Cl cycle is proposed to decrease electrical work requirement of the cycle and make it a more feasible one, and compete with the conventional water electrolysis (Ozcan and Dincer, 2015c). The selection of the newly developed four-step cycle is made related to following reasons:

- It is possible to obtain dry HCl gas by decomposing MgOHCl which leads to dry HCl electrolysis. Considering the practical voltage requirements, this option directly reduces the electrical work

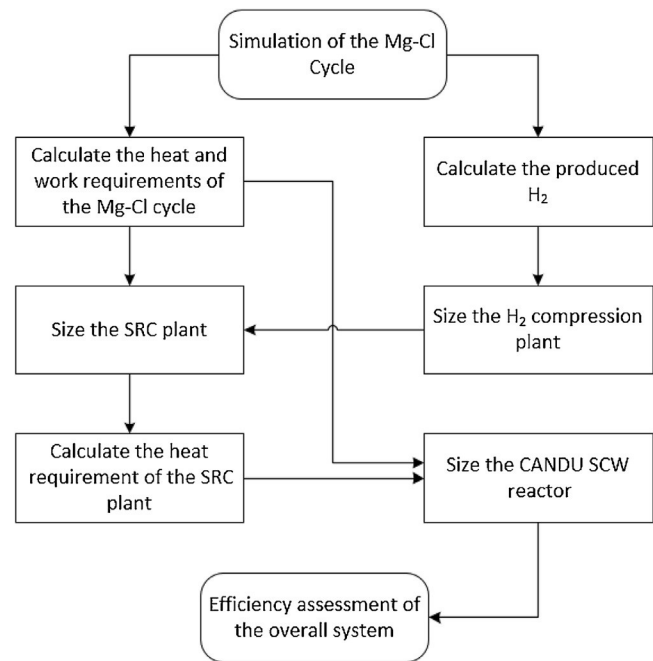


Fig. 1. Flowchart for the thermodynamic assessment of the integrated system.

consumption by 11.2%. This value is obtained from the ratio of Gibbs free energy of aqueous and anhydrous HCl electrolysis.

- The stoichiometry to produce same amount of hydrogen as in the Mg-Cl-B option can be reduced from two to one, by capturing the HCl gas in the decomposition step.
- MgO produced from high temperature hydrolysis is less reactive with the chlorine gas and has less surface area for proper reaction than hydrolysis of Mg(OH)₂. However, experimental studies showed that fine MgO can be produced from decomposition of MgOHCl which would enhance the reactivity of MgO with the chlorine gas (Kashani-Nejad et al., 2005, 2004; Hesson, 1979).
- The only endothermic reaction is decomposition of MgOHCl, and maximum temperature of the reaction can be reduced to 450 °C by using an inert gas (Nitrogen or Argon) to remove HCl gas from the surface of MgO particles. This also leads to a very fast conversion of the feed into desired products. The lower maximum temperature provides the option to link this cycle to lower temperature heat sources.

Here, the four-step cycle also carries the potential to decrease the electrical work consumption further by considering an HCl capture process after hydrolysis (Ozcan, 2015). This process is also included in the analysis by making a simple assumption of 30% HCl capture from the separation process. The results for this assumption are included in the performance assessment of the overall system.

System integration and preparation of produced hydrogen for end user have not previously been modeled or studied for the Mg-Cl cycle. Thus, system development with nuclear and renewable resources are essentially considered and performed for a comprehensive model. Various configurations of other possible thermal systems are integrated into this Mg-Cl cycle to provide required energy and to utilize the products of this cycle. Thus, this study thermodynamically investigates the overall performance of such an integrated system holistically by considering irreversibilities through the power production, hydrogen production and hydrogen treatment subsystems and comparatively discuss potential improvement options for a large capacity integrated system.

Table 1

Cycle options and individual reactions of the Mg–Cl cycle (Ozcan and Dincer, 2014b).

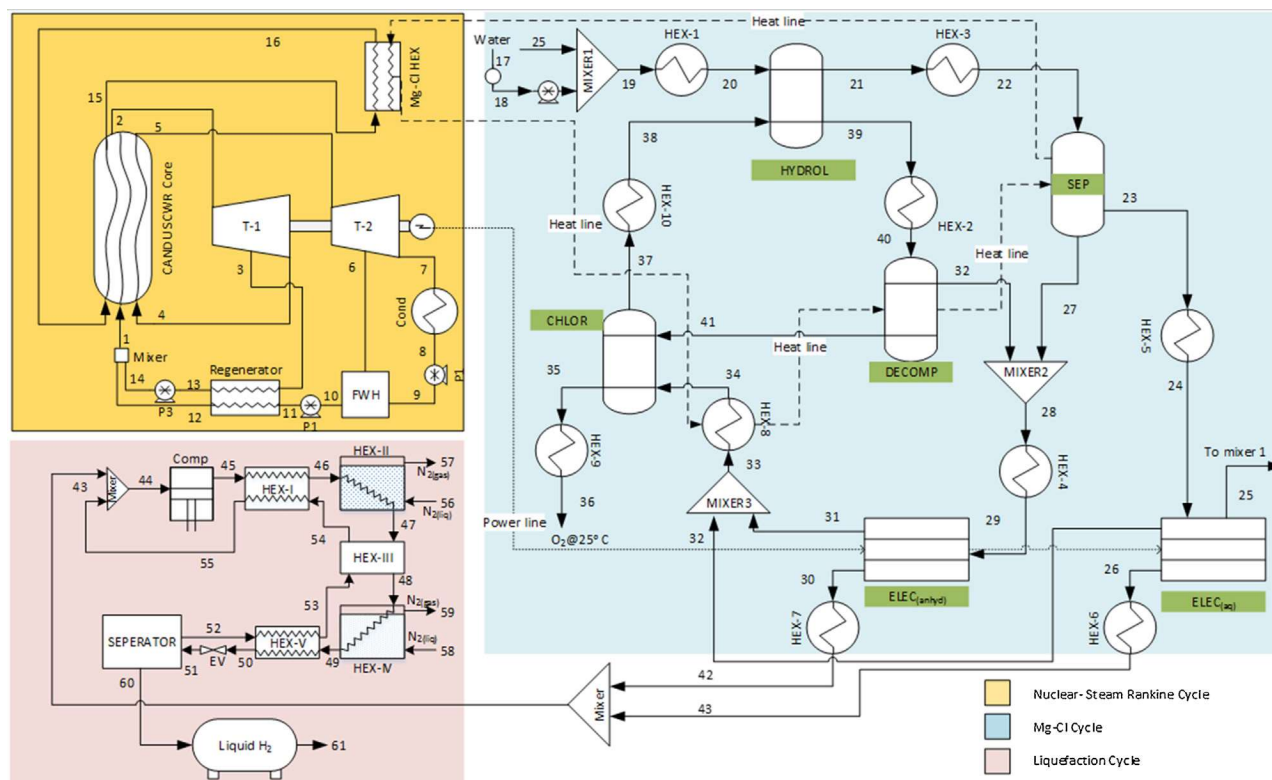
Cycle	Max temp (°C)	Reactions	Remarks
Mg–Cl-A	537	H: $\text{MgCl}_2 + \text{H}_2\text{O} \rightarrow \text{MgO} + 2\text{HCl}_{(\text{aq})}$ C: $\text{MgO} + \text{Cl}_2 \rightarrow \text{MgCl}_2 + 1/2\text{O}_2$ E: $2\text{HCl}_{(\text{aq})} \rightarrow \text{Cl}_2 + \text{H}_2(1.8\text{V})$	HCl production occurs in mixture with steam. MgO from hydrolysis is less reactive with chlorine and low particle surface area. The only endothermic reaction is hydrolysis.
Mg–Cl-B	500	H: $2\text{MgCl}_2 + 2\text{H}_2\text{O} \rightarrow 2\text{MgOHCl} + 2\text{HCl}_{(\text{aq})}$ C: $2\text{MgOHCl} + \text{Cl}_2 \rightarrow 2\text{MgCl}_2 + \text{H}_2\text{O} + 1/2\text{O}_2$ E: $2\text{HCl}_{(\text{aq})} \rightarrow \text{Cl}_2 + \text{H}_2(1.8\text{V})$	For the same amount of HCl production, stoichiometry of hydrolysis should be doubled. The only endothermic reaction is chlorination.
Mg–Cl-C	450	H: $\text{MgCl}_2 + \text{H}_2\text{O} \rightarrow \text{MgOHCl} + \text{HCl}_{(\text{aq})}$ D: $\text{MgOHCl} \rightarrow \text{MgO} + \text{HCl}_{(\text{g})}$ C: $\text{MgO} + \text{Cl}_2 \rightarrow \text{MgCl}_2 + 1/2\text{O}_2$ E: $\text{HCl}_{(\text{g})} \rightarrow 1/2\text{Cl}_2 + 1/2\text{H}_2(1.4\text{V})$ E: $\text{HCl}_{(\text{aq})} \rightarrow 1/2\text{Cl}_2 + 1/2\text{H}_2(1.8\text{V})$	The only endothermic reaction is decomposition step with higher heat requirement. A gas removing agent is required to separate HCl from MgO surface. Half of the HCl can be produced in dry form.

2. System description

An assessment of the system is made by following some consecutive steps. Initially, design of the Mg–Cl cycle is performed, and required heat and work requirements are calculated. The work requirement of the compression plant is also determined by considering the total H₂ produced from the Mg–Cl cycle. The steam Rankine cycle is then sized considering the total work requirement, where the nuclear reactor sizing is made considering total heating requirement of the Mg–Cl cycle and the SRC plant, as shown in Fig. 1. A detailed schematic diagram of the proposed system with state points is illustrated in Fig. 2. Here, the following state point ranges are used to evaluate thermodynamic properties of subsystems for system performance assessment:

- 1–16: Nuclear Rankine cycle
- 17–43: Mg–Cl cycle
- 44–61: Linde–Hampson hydrogen liquefaction cycle

CANDU super critical water reactor (SCWR) is used as the main energy resource as heat provider for the Mg–Cl cycle and Rankine cycle. Rankine cycle is modeled with regeneration and reheat option for enhanced cycle performance. Nuclear heat is used to superheat steam at high pressure and steam is first expanded to an assumed extraction pressure. Here, the stream is split into two with a ratio (f_1) which is then determined by writing a balance equation for the regenerator. Remaining steam is further expanded to another assumed expansion pressure, and reheated in the nuclear reactor. Same procedure for expansion is followed by providing a fraction of stream for open feed water heater (FWH). Finally, steam is extracted to vacuum pressure and condensed. After the first pump, water is mixed with steam from second turbine for heat recovery purpose, and mixture is assumed to be totally liquid. Fraction of stream splitting (f_2) is calculated based on energy balance of FWH. Further pumping is provided by the second pump, and heat is gained from regenerator. It is important that heat supply stream for the regenerator is again at condensed form for pumping to boiler pressure. A mixing chamber is then used to mix all streams

**Fig. 2.** Schematic of the integrated system.

and fed into nuclear reactor. One of the main issues to be pointed out is assumptions for extraction pressures. A simple optimization process for optimum extraction pressures are carried out where maximization of cycle energy efficiency is aimed (Klein and Nellis, 2012).

In this system, external heat requirement of the Mg–Cl cycle is also compensated by the nuclear reactor with a simple heat exchanger at a desired temperature range. Heat from reactor is than provided to heat requiring components of the Mg–Cl cycle. Required water and recovered steam from the cycle are fed to hydrolysis reactor after heated up to necessary reactor temperature and formation of MgOHCl and Steam/HCl mixture is accomplished. MgOHCl is reacted into fine MgO and dry HCl by the decomposition reactor, and fine MgO is reacted with the chlorine gas from electrolysis step in the chlorination reactor. An assumed amount of HCl is separated from steam in the separation unit, and dry HCl is fed to dry electrolysis cell, where the remaining is electrolysed in the aqueous electrolysis cell. Separation process is based on HCl capture on MgO, and liberation is made at higher temperature with three subsequent chemical processes.

Since the produced hydrogen is at ambient conditions, storage is considered to be hydrogen liquefaction. This cycle is relatively more energy intensive than compression, however, density of liquid hydrogen is almost $\sim 1120 \text{ kg/m}^3$ and it is 29 times better than compressed hydrogen at 700 bar, in terms of volume occupation. Thus, a Linde–Hampson liquefaction plant, with a secondary nitrogen cooling is considered for hydrogen storage (Nandi and Sarangi, 1993; Bracha et al., 1994; Dincer and Kanoglu, 2011). Since the plant is developed to produce 1 kmole/s hydrogen, an initial assumption is made based on the amount of produced liquid hydrogen. Power consumption of the plant and nitrogen cooling process is than determined based on the yield of liquid hydrogen. Hydrogen from the Mg–Cl cycle and remaining hydrogen from liquefaction is mixed and compressed to a specific pressure. An initial internal cooling is made by releasing heat to returning hydrogen from separator, and two stage cooling of hydrogen is made using liquid nitrogen as a secondary heat transfer fluid. Heat exchanging processes decrease the temperature of hydrogen down to its critical point, where liquefaction is obtained after expansion valve. Liquefied hydrogen is then stored for transportation. The unique product of the overall integrated system is liquid hydrogen.

The modeling studies of reactors are constructed and performed based on the Aspen plus simulation package. There are several reactor blocks in Aspen plus to simulate reactions in different ways. In order to simulate a known stoichiometric reaction where the product conversions are not taken into account, the stoichiometric type (RStoic) reactors are potentially used. These reactors are then proposed a good selection to determine reaction heats and thermodynamic properties of input and outputs of the reaction. For a reaction with negligible reaction kinetics which can be in one or more phases can be simulated using several built in reactor models (Rgibbs, REquil and Ryield). Here, RGibbs type reactor aims to minimize the Gibbs free energy of the reaction which is a promising built-in reactor type to find out reaction conditions in a feasible way. For a known yield of a reaction at a specific reaction condition, the RYield type reactors are conveniently used to determine thermochemical and thermodynamic properties of inlet and outlet streams, as well as the corresponding reaction heat. The RBatch, RCstr and RPlug reactor types give reliable practical results by considering both stoichiometry and experimentally derived kinetics of a reaction. Such rigorous type reactors are then used for reactions which are experimentally studied with the obtained kinetic parameters. Other details of all built-in reactor types and user models can be found in user guides of Aspen Plus software (Aspen plus user guide, 2003). The results from Aspen Plus software are transferred to Engineering Equation Solver (EES) software to integrate

the results with other subsystems to evaluate the overall performance characteristics of the integrated system.

3. Modeling and assessment

The mass, energy, entropy and exergy balances are required in the first step of the energy and exergy analyses to determine the heat input/output, entropy generation rate, exergy destructions, and energy and exergy efficiencies. The mass balance equation for a steady-state condition is written as follows:

$$\sum \dot{m}_{\text{in}} = \sum \dot{m}_{\text{out}} + \frac{dm_{\text{CV}}}{dt} \quad (1)$$

where the second definition at the right side is cancelled when the flow is steady. Energy balance of a system can be defined by considering all forms of energy within a system

$$\Delta E_{\text{sys}} = m \Delta e_{\text{sys}} = m \left[\left(u_{\text{out}} + \frac{1}{2} v_{\text{out}}^2 + gz_{\text{out}} \right) - \left(u_{\text{in}} + \frac{1}{2} v_{\text{in}}^2 + gz_{\text{in}} \right) \right] \quad (2)$$

where u stands for internal energy, v is velocity of the corresponding flow, g is gravity and z is height. Energy of a non-flowing thermodynamic system is defined as

$$e = u + \frac{1}{2} v^2 + gz \quad (3)$$

The total energy of a flowing matter can be defined as sum of non-flow energy and flow work:

$$\theta = e + Pv \quad (4)$$

The energy balance of an open system can now be defined as follows:

$$\begin{aligned} \sum \dot{m} \theta + \sum \dot{Q}_{\text{in}} + \sum \dot{W}_{\text{in}} \\ = \sum \dot{m} \theta + \sum \dot{Q}_{\text{out}} + \sum \dot{W}_{\text{out}} + \left[\frac{d(me)}{dt} \right]_{\text{sys}} \end{aligned} \quad (5)$$

where the fourth definition at the right side is cancelled when the flow is steady. When kinetic and potential energies are cancelled, sum of internal energy and flow work correspond to enthalpy of the individual stream.

The heat transfer for a chemical process is basically difference between enthalpies of products and reactants of a reaction and is determined with the following expression:

$$Q = H_P - H_R = \sum n_p (\bar{h}_f^\circ + \bar{h} + \bar{h}^\circ)_p - \sum n_R (\bar{h}_f^\circ + \bar{h} + \bar{h}^\circ)_R \quad (6)$$

where n refers to molar amount, and corresponding h values are enthalpy of formation, enthalpy of state, and reference enthalpy, respectively. Enthalpy of formation and reference enthalpy values can be found in thermochemical tables of various databases, where enthalpy of state is generally calculated based on temperature of the reaction with various empirical correlations. Supposing that the reactants of considered reaction are A , and B , and products are denoted as C , and D ; the specific heat of the individual component is expressed as follows (Kelley, 1945):

$$Cp_i = a_i + b_i T + c_i T^{-2} \quad (7)$$

where a , b and c are empirically calculated constants. The specific heat for the individual reaction depends on the specific heats of the individual components of the reaction, and is defined as follows:

$$\Delta Cp = Cp_c + Cp_d - Cp_a + Cp_b = a + bT + cT^{-2} \quad (8)$$

Here, the empirically calculated constants are also calculated as the difference of the products and reactants in a general form. Corresponding reaction heat can be calculated in terms of temperature with the standard heat of the reaction as follows:

$$\Delta H = \int \Delta C_p dT = \Delta H_0 + aT + \frac{b}{2} T^2 - \frac{c}{T} \quad (9)$$

The entropy balance of an open system can be expressed in rate form as sum of entropy input and generated entropy is equal to sum of output entropy and change of control volume entropy as follows:

$$\sum \dot{S}_{in} + \dot{S}_{gen} = \sum \dot{S}_{out} + \frac{dS_{sys}}{dt} \quad (10)$$

If there is heat transfer across the boundary of a control volume, than the balance equation becomes

$$\sum_{in} \dot{m}s + \sum_{in} \int \frac{d\dot{Q}}{T} + \dot{S}_{gen} = \sum_{out} \dot{m}s + \sum_{out} \int \frac{d\dot{Q}}{T} + \left[\frac{d(S)}{dt} \right]_{cv} \quad (11)$$

where the above equation can be further simplified by considering a steady and adiabatic process:

$$\sum_{in} \dot{m}s + \dot{S}_{gen} = \sum_{out} \dot{m}s \quad (12)$$

When the entropy difference of a reaction is required for chemical processes, it can be calculated using Gibbs free energy and heat of the reaction as follows

$$\Delta S = \frac{\Delta H - \Delta G^0}{T} = a + alnT + bT - \frac{c}{2} T^{-2} - I \quad (13)$$

where ΔG^0 is determined with the following expression

$$\Delta G^0 = \int \frac{\Delta H}{T^2} dT = \Delta H_0 - aTlnT - \frac{b}{2} T^2 - \frac{c}{2T} + IT \quad (14)$$

where I corresponds to irreversibility, and can be determined from total entropy generation and ambient temperature. For the known values of standard heat of reaction and I , temperature is the ultimate variable to calculate the free energy of the reaction. The free energy is also related with the equilibrium constant (K) as follows:

$$\Delta G^0 = -RTlnK \quad (15)$$

where K is defined as the rate of activities of the products and reactants as follows:

$$K = \frac{\alpha_c \alpha_d}{\alpha_a \alpha_b} \quad (16)$$

The activities of the gaseous and liquid reactants and products can be taken as their partial pressures dependent on the reference pressure. Thus, the equilibrium constant can be defined as:

$$K = \left(\frac{p_c p_d}{p_a p_b} \right) \frac{1}{p^0} \quad (17)$$

Here, p^0 is the reference pressure considered for calculation and for its effects on the behavior of the reaction. The calculations and the amounts of the produced components are based on the free energy of the reactions. In order to obtain a favorable reaction in terms of pressure and temperature of the reactions, determination of the molar percentages of the produced gaseous components should be conducted. Specific heat equations for some of the required substances through the Mg–Cl cycle are tabulated in Table 2.

Note that the exergy of a non-flow system is sum of all forms of exergy, and flow exergy is sum of non-flow exergy and flow work as expressed below

$$Ex_{nf} = Ex_{ph} + Ex_{kin} + Ex_{pot} + Ex_{ch} \quad (18)$$

$$Ex_f = Ex_{nf} + (P - P_0)V \quad (19)$$

Table 2
Specific heat equations for some substances (Kelley, 1945).

Substance	Specific heat equation (cal mole ⁻¹ C ⁻¹)
MgO	$10.86 + 1.197 \times 10^{-3}T - 2.087 \times 10^5 T^{-2}$
MgCl _{2(s)}	$18.9 + 1.42 \times 10^{-3}T - 2.06 \times 10^5 T^{-2}$
MgCl _{2(l)}	22.1
MgCl ₂ H ₂ O	$21.75 + 19.45 \times 10^{-3}T$
MgOHCl	$13.40 + 14.47 \times 10^{-3}T$

Table 3
Standard chemical exergy of chemical species in Mg–Cl cycle (Kotas, 2013).

Substance	\bar{ex}_{ch}^0 (kJ/kmol)	Substance	\bar{ex}_{ch}^0 (kJ/kmol)
H ₂ O _(g)	11,710	HCl(g)	85,950
H ₂ O _(l)	3120	O ₂ (g)	3970
MgCl _{2(s)}	151,860	Cl ₂ (g)	117,520
MgO _(s)	59,170	H ₂ (g)	238,490

The physical exergy of a stream is expressed as

$$Ex_{ph} = (U - U_0) + P_0(V - V_0) - T_0(S - S_0) \quad (20)$$

Here, U , V , and S are internal energy, volume, and entropy of a closed system. Kinetic and potential energies are associated directly with work, which remains the same in exergy definition as expressed in energy balance definitions. The chemical exergy of a system is expressed as

$$Ex_{ch} = \sum n_i (u_i^0 - u_i^{00}) \quad (21)$$

where u_i^0 is chemical potential of i_{th} component in thermomechanical equilibrium and u_i^{00} is chemical potential of i_{th} component in chemical equilibrium. Standard chemical exergy values of various chemical substances can be found elsewhere (Dincer and Rosen, 2012; Kotas, 2013). Table 3 represents standard chemical exergy values of some substances used through the Mg–Cl cycle.

For a control volume, exergy balance of a system can now be expressed as

$$\begin{aligned} & \sum_{in} [\dot{W} + \dot{m}ex + \dot{Ex}^Q] \\ &= \sum_{in} [\dot{W} + \dot{m}ex + \dot{Ex}^Q] + \frac{dEx}{dt} - \frac{P_0(dV_{CV})}{dt} + \dot{Ex}_d \end{aligned} \quad (22)$$

\dot{Ex}_d is exergy destruction and its associated with entropy generation rate as follows:

$$\dot{Ex}_d = T_0 \dot{S}_{gen} \quad (23)$$

\dot{Ex}^Q is exergy associated with heat transfer and expressed as

$$\dot{Ex}^Q = \left(1 - \frac{T_0}{T} \right) \dot{Q} \quad (24)$$

It should be noted that second and third definitions in Eq. (22) are cancelled when the system is steady flow. One can now perform efficiency assessments based on energy and exergy of any system by simply considering inputs and outputs to and from the system. Energy and exergy efficiencies are expressed in a general form as follows:

$$\eta_{en} = \frac{\text{Usefuloutput}}{\text{Total input}} \quad (25)$$

$$\eta_{ex} = \frac{Ex_{useful}}{Ex_{in}} = 1 - \frac{\dot{Ex}_d}{Ex_{in}}$$

Table 4
Balance equations for the SRC subsystem.

Component	Balance equations
Reactor	$\dot{m}_1 = \dot{m}_2 + \dot{m}_4 + \dot{m}_5$ $\dot{E}_1 + \dot{E}_4 + \dot{Q}_{in} = \dot{E}_2 + \dot{E}_5$ $\dot{S}_1 + \dot{S}_4 + \dot{S}_{gen} + \frac{\dot{Q}_{in}}{T_r} = \dot{S}_2 + \dot{S}_5$ $\dot{Ex}_1 + \dot{Ex}_4 + \dot{Ex}^{Q_{in}} = \dot{Ex}_2 + \dot{Ex}_5 + \dot{Ex}_{dest}$
Turbine I	$\dot{m}_2 = \dot{m}_3 + \dot{m}_4$ $\dot{E}_2 = \dot{E}_3 + \dot{E}_4 + \dot{W}_{t1}$ $\dot{S}_2 + \dot{S}_{gen} = \dot{S}_3 + \dot{S}_4$ $\dot{Ex}_2 = \dot{Ex}_3 + \dot{Ex}_4 + \dot{W}_{t1} + \dot{Ex}_{dest}$
Turbine II	$\dot{m}_5 = \dot{m}_6 + \dot{m}_7$ $\dot{E}_5 = \dot{E}_6 + \dot{E}_7 + \dot{W}_{t2}$ $\dot{S}_5 + \dot{S}_{gen} = \dot{S}_6 + \dot{S}_7$ $\dot{Ex}_5 = \dot{Ex}_6 + \dot{Ex}_7 + \dot{W}_{t2} + \dot{Ex}_{dest}$
FWH	$\dot{m}_6 + \dot{m}_9 = \dot{m}_{10}$ $\dot{E}_6 + \dot{E}_9 = \dot{E}_{10}$ $\dot{S}_6 + \dot{S}_9 + \dot{S}_{gen} = \dot{S}_{10}$ $\dot{Ex}_6 + \dot{Ex}_9 = \dot{Ex}_{10} + \dot{Ex}_{dest}$
Regenerator	$\dot{m}_{11} = \dot{m}_{12}, \dot{m}_3 = \dot{m}_{13}$ $\dot{E}_{11} + \dot{E}_3 = \dot{E}_{12} + \dot{E}_{13}$ $\dot{S}_{11} + \dot{S}_3 + \dot{S}_{gen} = \dot{S}_{12} + \dot{S}_{13}$ $\dot{Ex}_{11} + \dot{Ex}_3 = \dot{Ex}_{12} + \dot{Ex}_{13} + \dot{Ex}_{dest}$
Condenser	$\dot{m}_7 = \dot{m}_8$ $\dot{E}_7 = \dot{E}_8 + \dot{Q}_{out}$ $\dot{S}_7 + \dot{S}_{gen} = \dot{S}_8 + \frac{\dot{Q}_{out}}{T_c}$ $\dot{Ex}_7 = \dot{Ex}_8 + \dot{Ex}^{Q_{out}} + \dot{Ex}_{dest}$
Pumps	$\dot{m}_i = \dot{m}_o$ $\dot{E}_i + \dot{W}_c = \dot{E}_o$ $\dot{S}_i + \dot{S}_{gen} = \dot{S}_o$ $\dot{Ex}_i + \dot{W}_c = \dot{Ex}_o + \dot{Ex}_{dest}$

In addition, another performance characteristics can be given for the liquid hydrogen yield from the Linde–Hampson plant as follows (Nandi and Sarangi, 1993).

$$y = \frac{h_{54} - h_{57}}{h_{54} - h_{60}} \quad (26)$$

The equations given above are applied to the proposed integrated system for one case study for performance assessment and to determine locations of irreversibilities throughout the system. Efficiency definitions for subsystems and the overall system can now be defined based on the basic thermodynamic concepts.

3.1. Nuclear heated steam Rankine cycle

The steam Rankine cycle is designed as a four-stage-turbine system with extraction of some heat in order to provide reheating before boiling the stream where boiler of the cycle is taken to be the SCWR. The ratio of stream 3 is defined as f_1 and remaining is sent for reheating ($1-f_1$). As for the second extraction, this ratio

is defined as $(1-f_1)f_2$ and remaining as $(1-f_1)(1-f_2)$. The energy balance of the feed water heater is used to calculate f_2 as follows (Klein and Nellis, 2012):

$$(1-f_1)f_2\dot{m}_w h_6 + (1-f_1)(1-f_2)\dot{m}_w h_9 = (1-f_1)\dot{m}_w h_{10} \quad (27)$$

Dividing the equation by $(1-f_1)$:

$$\dot{f}_2 h_6 + (1-f_2)\dot{m}_w h_9 = h_{10} \quad (28)$$

The ratio of steam extracted from the first turbine is calculated using the energy balance of the regenerator as follows:

$$f_1 h_3 + (1-f_1)h_{11} = f_1 h_{13} + (1-f_1)h_{12} \quad (29)$$

At the beginning of the analysis of the steam power plant, the highest pressure and the condensing pressure are set to constant values, and extraction pressures of the turbines are guessed. After obtaining energy and exergy efficiencies of the system, these values are optimized by maximizing energy and/or exergy efficiency. The constraints for the optimization and equations to calculate the optimized fraction of the extraction pressures (y_1, y_2, y_3) are defined as follows:

$$P_2 > P_3 > P_4 > P_6 > P_7 \quad (30)$$

subjected to

$$P_3 = P_2 - y_1(P_2 - P_7) \quad (31)$$

$$P_5 = P_3 - y_2(P_3 - P_7) \quad (32)$$

$$P_6 = P_5 - y_2(P_5 - P_7) \quad (33)$$

The energy and exergy efficiencies of the nuclear – SRC are defined as follows:

$$\eta_{en,RC} = \frac{\dot{W}_{turbines} - \dot{W}_{pumps}}{\dot{Q}_b + \dot{Q}_{rht}} \quad (34)$$

$$\eta_{ex,RC} = \frac{\dot{W}_{turbines} - \dot{W}_{pumps}}{\dot{Ex}_1 + \dot{Ex}_4 - \dot{Ex}_{R2} - \dot{Ex}_5} \quad (35)$$

The balance equations required to determine component based characteristics of the SRC system are tabulated in Table 4.

3.2. Hydrogen liquefaction subsystem

The Linde–Hampson liquefaction plant is designed to liquefy all the hydrogen from the Mg–Cl cycle. Thus, liquefied hydrogen rate is set to a constant value and determination of the total mass flow of hydrogen is made based on this assumption. For this purpose, the yield of the liquid hydrogen should be known as suggested by Nandi and Sarangi (1993) and can be calculated by solving below equations:

$$y = (h_{53} - h_{49})/(h_{53} - h_{60}) \quad (36)$$

and

$$h_{46} = h_{45} - (1-y)(h_{55} - h_{54}) \quad (37)$$

$$h_{55} = h_{54} + \varepsilon_{hex}(h_{55} - h_{54}) \quad (38)$$

$$h_{48} = h_{47} - (1-y)(h_{54} - h_{53}) \quad (39)$$

$$h_{54} = h_{53} + \varepsilon_{hex}(h_{54} - h_{53}) \quad (40)$$

$$h_{53} = h_g + \varepsilon_{hex}(h_{53} - h_g) \quad (41)$$

$$h_{50} = h_{49} - (1-y)(h_{52} - h_g) \quad (42)$$

$$h_{51} = h_{50} \quad (43)$$

where ε_r is the heat exchanger effectiveness factor and states with indices are values for effectiveness of 1. For an assumed yield, it is possible to calculate enthalpy values of streams which

Table 5
Assumptions and system parameters for the integrated system.

Variable	Symbol	Unit	Range
SRC system			
Turbine inlet temperature	TIT	K	750–900
High pressure side	Ph	bar	90–110
Turbine efficiency	η_t	%	85
Pump efficiency	η_p	–	80
Approach temperature	ΔT_{app}	°C	10–15
Initial extraction pressure fraction	y	–	0.5
Liquefaction system			
Operating pressure	Ph	bar	7.5–15
N ₂ bath temperature	–	K	65–75
Heat exchanger effectiveness	ε	–	0.85–1
Hydrogen liquefaction temperature	–	K	23

Table 6

Component based balance equations for the Linde–Hampson hydrogen liquefaction plant.

Component	Balance equations
Compressor	$\dot{m}_{44} = \dot{m}_{45}$ $\dot{E}_{44} + \dot{W}_c = \dot{E}_{45}$ $\dot{S}_{44} + \dot{S}_{gen} = \dot{S}_{45}$ $\dot{Ex}_{44} + \dot{W}_c = \dot{Ex}_{45} + \dot{Ex}_{dest}$
Hex-1	$\dot{m}_{45} = \dot{m}_{46}; \dot{m}_{54} = \dot{m}_{55}$ $\dot{E}_{45} + \dot{E}_{54} = \dot{E}_{46} + \dot{E}_{55}$ $\dot{S}_{45} + \dot{S}_{54} + \dot{S}_{gen} = \dot{S}_{46} + \dot{S}_{55}$ $\dot{Ex}_{45} + \dot{Ex}_{54} = \dot{Ex}_{46} + \dot{Ex}_{55} + \dot{Ex}_{dest}$
Hex-2	$\dot{m}_{46} = \dot{m}_{47}; \dot{m}_{56} = \dot{m}_{57}$ $\dot{E}_{46} + \dot{E}_{56} = \dot{E}_{47} + \dot{E}_{57}$ $\dot{S}_{46} + \dot{S}_{56} + \dot{S}_{gen} = \dot{S}_{47} + \dot{S}_{57}$ $\dot{Ex}_{46} + \dot{Ex}_{56} = \dot{Ex}_{47} + \dot{Ex}_{57} + \dot{Ex}_{dest}$
Hex-3	$\dot{m}_{47} = \dot{m}_{48}; \dot{m}_{53} = \dot{m}_{54}$ $\dot{E}_{47} + \dot{E}_{53} = \dot{E}_{48} + \dot{E}_{54}$ $\dot{S}_{47} + \dot{S}_{53} + \dot{S}_{gen} = \dot{S}_{48} + \dot{S}_{54}$ $\dot{Ex}_{47} + \dot{Ex}_{53} = \dot{Ex}_{48} + \dot{Ex}_{54} + \dot{Ex}_{dest}$
Hex-4	$\dot{m}_{48} = \dot{m}_{49}; \dot{m}_{58} = \dot{m}_{59}$ $\dot{E}_{48} + \dot{E}_{58} = \dot{E}_{49} + \dot{E}_{59}$ $\dot{S}_{48} + \dot{S}_{58} + \dot{S}_{gen} = \dot{S}_{49} + \dot{S}_{59}$ $\dot{Ex}_{48} + \dot{Ex}_{58} = \dot{Ex}_{49} + \dot{Ex}_{59} + \dot{Ex}_{dest}$
Hex-5	$\dot{m}_{49} = \dot{m}_{50}; \dot{m}_{52} = \dot{m}_{53}$ $\dot{E}_{49} + \dot{E}_{52} = \dot{E}_{50} + \dot{E}_{53}$ $\dot{S}_{49} + \dot{S}_{52} + \dot{S}_{gen} = \dot{S}_{50} + \dot{S}_{53}$ $\dot{Ex}_{49} + \dot{Ex}_{52} = \dot{Ex}_{50} + \dot{Ex}_{53} + \dot{Ex}_{dest}$
Separator	$\dot{m}_{51} = \dot{m}_{52} + \dot{m}_{60}$ $\dot{E}_{51} = \dot{E}_{52} + \dot{E}_{60}$ $\dot{S}_{51} + \dot{S}_{gen} = \dot{S}_{52} + \dot{S}_{60}$ $\dot{Ex}_{51} = \dot{Ex}_{52} + \dot{Ex}_{60} + \dot{Ex}_{dest}$

leads to determination of the compression power requirement for both hydrogen and nitrogen. The work requirement for nitrogen is assumed to be 7760 kJ/kg N₂. The amount of nitrogen requirement is calculated based on the enthalpy difference of heat exchangers II and IV and the mass flow rate of the hydrogen in the cycle.

The assumptions and ranges of variations for the liquefaction cycle, as well as for the SRC subsystems are provided in Table 5. Since the main inputs to the cycle are hydrogen and power for compression of nitrogen and hydrogen, these amounts are taken to be the denominator for performance calculations.

The main output from the system is liquid hydrogen. Thus, energy and exergy efficiencies of the cycle can be determined as follows:

$$\eta_{en,LH} = \frac{\dot{E}_{h2,l}}{\dot{E}_{H2,g} + \dot{W}_{c,H2} + \dot{W}_{c,N2}} \quad (44)$$

$$\eta_{ex,LH} = \frac{\dot{Ex}_{h2,l}}{\dot{Ex}_{H2,g} + \dot{W}_{c,H2} + \dot{W}_{c,N2}} \quad (45)$$

Table 7

Heat exchanger information to build composite curves.

	Component	Supply temperature (°C)	Target temperature (°C)	Duty (MW)	Cp (MW/°C)
Cold	Hex-1	66	280	546.8	2.55
	Hex-2	280	450	7.8	0.045
	Hex-4	70	450	11.2	0.029
	Hex-7	70	500	15.61	0.036
	Hex-1c	275	350	4.14	0.055
	Hex-2c	350	450	4.7	0.047
Hot	Hex-3	275	70	483.8	2.36
	Hex-5	70	25	0.65	0.014
	Hex-6	70	25	0.65	0.014
	Hex-8	500	25	7.46	0.016
	Hex-9	500	280	17.8	0.081
	Hex-3c	450	280	8.11	0.048

Finally, overall efficiency assessment of the integrated system is performed by considering liquid hydrogen from the Linde–Hampson cycle, and oxygen from the Mg–Cl cycle, and calculated for energy and exergy efficiencies as follows:

$$\eta_{en,SII} = \frac{\dot{E}_{h2,l} + \dot{E}_{o2}}{\dot{Q}_b + \dot{Q}_{rht} + \dot{Q}_{mgcl}} \quad (46)$$

$$\eta_{ex,SII} = \frac{\dot{Ex}_{h2,l} + \dot{Ex}_{o2}}{\dot{Ex}^{Q_b} + \dot{Ex}^{Q_{rht}} + \dot{Ex}^{Q_{mgcl}}} \quad (47)$$

The balance equations of the liquefaction cycle are tabulated in Table 6 in order to evaluate component based characteristics of the cycle.

3.3. Pinch point analysis

Both endothermic and exothermic heat exchangers are coupled for internal heat recovery with a simple assumption of 85% heat exchanger effectiveness for the Mg–Cl cycle. However, it is of importance to conduct a proper pinch point analysis in order to evaluate maximum possible heat recovery, as well as the amount and grade of the required heat. As for the final design, 10 °C of approach temperature is assumed for the pinch point analysis and all heat exchangers through the cycle are included in the calculation. Specific heats of the streams are taken from the Aspen Plus simulation results and calculation is made by multiplication of the mass flow rates and average specific heats of the corresponding streams. The required information and data to build the composite curves of the cycle are summarized in Table 7.

4. Results and discussion

For the proposed system, produced hydrogen is liquefied using Linde–Hampson liquefaction cycle, and power requirement is compensated by a steam Rankine cycle energized by CANDU SCWR reactor. With the known heat and power requirements of Mg–Cl cycle, power consumption of the liquefaction cycle is also determined.

4.1. Mg–Cl cycle subsystem

A comprehensive thermodynamic analysis of the four-step Mg–Cl cycle with HCl capture is conducted for 1 kmole/s hydrogen producing plant. Table 8 summarizes the endothermic and exothermic reactions, as well as heat exchanger loads. The practical voltage requirement of the aqueous and anhydrous HCl electrolysis is taken to be 1.8 V, and 1.4 V, respectively. The highest heat requiring component is the Hex-1, where phase change and superheating for a large amount of water (11 kmole/s) is required. However, Hex-3 recovers most of this heat with its high heat load. The total heat

Table 8

Energy balance of the four-step Mg–Cl cycle with HCl capture.

Component	Process	Temperature (°C)	ΔH (MJ/kmol H ₂)	\dot{W} (MW)
Hydrolysis	MgCl ₂ hydrolysis	280	17.82	–
Decomposition	MgOHCl decomposition	450	118.1	–
Chlorination	MgO chlorination	500	−31.51	–
HCl Separation ^a	–	280, 350, 450	17.77	–
Electrolysis (aq)	Aqueous HCl electrolysis	70	–	121.57
Electrolysis (dry)	Anhydrous HCl electrolysis	70	–	175.6
HEX-1	Steam superheating	280	546.8	–
HEX-2	MgOHCl heating	450	7.8	–
HEX-3	HCl _(aq) cooling	70	−483.8	–
HEX-4	HCl _(dry) cooling	70	11.2	–
HEX-5	Hydrogen cooling	25	−0.65	–
HEX-6	Hydrogen cooling	25	−0.65	–
HEX-7	Chlorine heating	500	15.61	–
HEX-8	Oxygen cooling	25	−7.46	–
HEX-9	MgCl ₂ cooling	280	−17.8	–
Auxiliary	Water pumping, inert gas compression	–	–	1.1
Total heat ^b	–	–	283.47	–
Total work	–	–	–	298.27

^a Total heat from three reactor separation.^b Total heat is calculated based on 85% of heat exchanger effectiveness, and exothermic reactions are not included in the calculation.

requirement for the overall cycle is calculated to be 283.5 MW, which is higher than previously evaluated values for stoichiometry. For 30% HCl capture assumption, an electrical energy requirement is 297.2 MW. This is almost 14.5% lower than direct aqueous HCl electrolysis (347.6 MW), and 6.7% lower than water electrolysis (~318 MW considering 1.65 V at 5 kA/m²).

A total assessment of the cycle can be made by evaluating total performance of the system. Energy and exergy efficiencies of this cycle correspond to 41.7%, and 50.6%, respectively. Amount of steam required for hydrolysis step is one of the main reasons of higher heat requirement. At stoichiometric conditions efficiency of the conventional cycle is evaluated as 55.2%. However, it is not wise to further assess the three-step cycles due to aqueous HCl electrolysis. Fig. 3 summarizes efficiency comparison of the four-step Mg–Cl cycle with and without HCl capture. Dry HCl capture increases the energy and exergy efficiencies of the system by 5.46%, and 8%, respectively. Considering a wider point of view, production of power is less efficient than production of heat. When energy supply subunits to this cycle are taken into account, less power requirement is expected to bring a more feasible integrated system in terms of performance. The maximum achievable energy and exergy efficiency values are 43.7%, and 53.66%, respectively, with full HCl capture from the proposed reaction couples.

The pinch point analysis results impose that the cycle shows lower external heat requirement than that of a simple calculation based on heat exchanger effectiveness factor. 115 MW energy is required from an external source to heat the cold streams, and the

rate of heating should be higher than 250 °C as presented in Fig. 4. The total heat requirement of the cycle now becomes 248.58 MW for 1 kmol/s hydrogen production. Using the result from pinch point analysis, energy and exergy efficiencies of the cycle becomes 44.3% and 53%, respectively. Further investigation can be performed by applying various heat exchanger networks for a more efficient heat recovery within the system.

4.2. Liquefaction cycle subsystem

The compression of hydrogen gas up to 700 bar with the aforementioned storage method increases the density of hydrogen to ~38 kg/m³. The liquefied hydrogen shows ~1121 kg/m³ density value which is almost 29 times more than storage at high pressure (700 bar). This option would make the transportation easier and cost effective. Thus, Linde–Hampson type hydrogen liquefaction plant is considered as the hydrogen storage subunit of the proposed system. State point information and T-s diagram of the cycle is represented in Table 9 and Fig. 5, respectively. An isothermal compression of hydrogen is made and individual heat exchangers are internally utilized to cool down the high pressure hydrogen down to its critical point. Liquid nitrogen is used to decrease the temperature down to 50 K, where an expansion valve is used to liquefy hydrogen at 23 K. Liquid hydrogen is collected at the bottom of the separator, where remaining gas conducts internal cooling and is fed back to compressor at ambient conditions.

Table 9

State point information for the Linde–Hampson hydrogen liquefaction plant.

State	T (K)	P (kPa)	h (kJ/kg)	s (kJ/kgK)	ex (MJ/kg)	Ex (MW)
43	298	101	3815	52.99	238.500	238.5
44	298	101	3815	52.99	238.500	1591
45	298	101	3850	34.84	243.799	1662
46	146.2	8080	1826	25.24	244.558	1672
47	77.5	8080	904	16.7	246.113	1693
48	71.81	8080	820.1	15.57	246.356	1700
49	65	8080	714.1	14.02	246.699	1701
50	45.36	8080	381.4	7.924	248.136	1720
51	20.36	8080	381.4	18.73	245.001	1678
52	20.36	101	448.6	22.04	244.110	1417
53	56.81	101	840	33.16	241.277	1387
54	66.22	101	938.8	34.76	240.909	1379
55	288	101	3320	52.99	238.005	1343
60	20.36	101	381.4	18.73	245.001	251.5

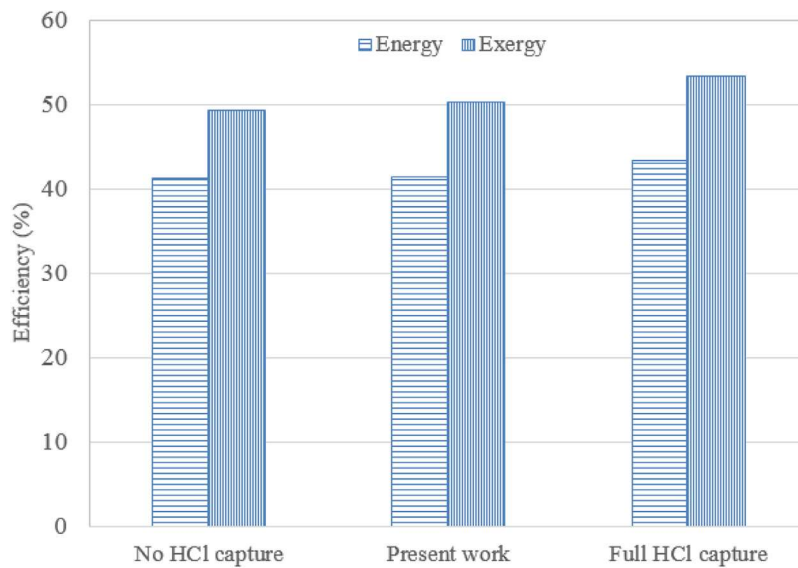


Fig. 3. Comparison of energy and exergy efficiencies of the modified four-step cycle with and without HCl capture.

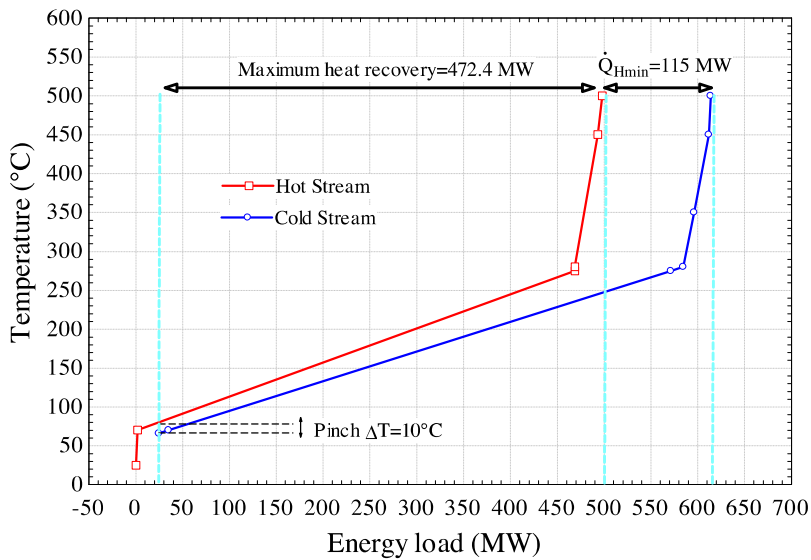


Fig. 4. Composite curves of the modified MgCl-C cycle.

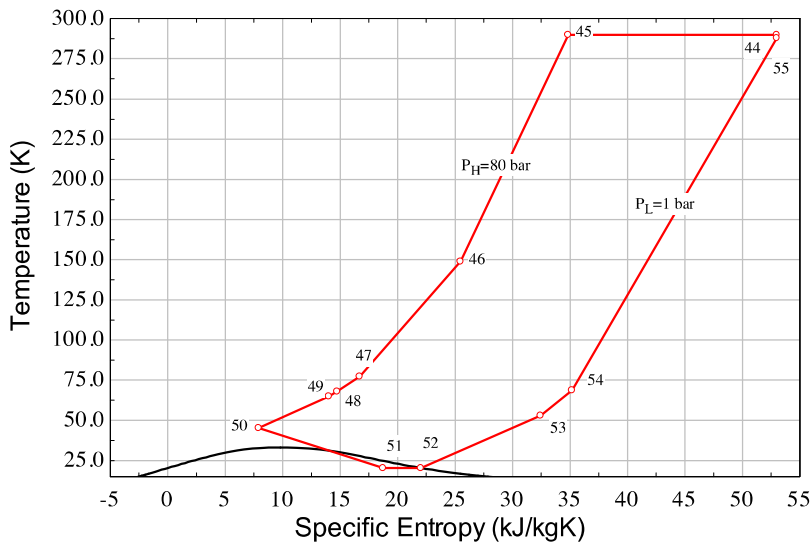


Fig. 5. T-S diagram of the precooled Linde–Hampson hydrogen liquefaction plant.

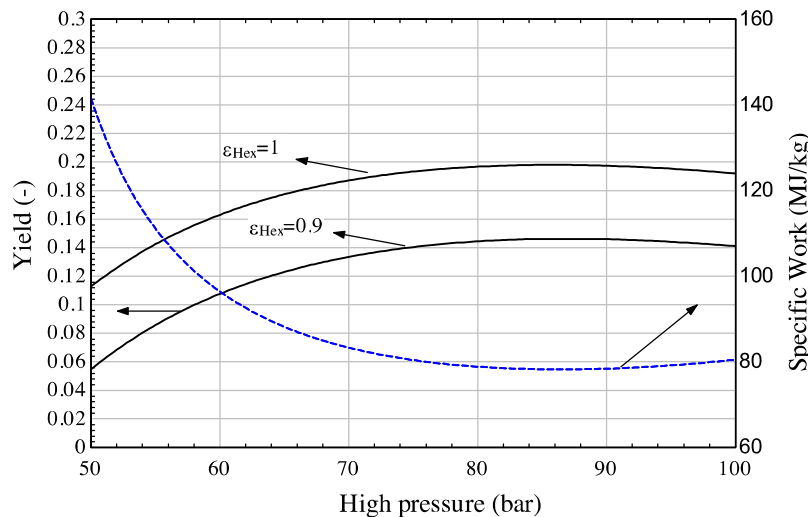


Fig. 6. Effect of compression pressure on liquid hydrogen yield and specific work consumption of the cycle.

Since heat exchangers play a crucial role on liquefaction, and compression pressure is an influential factor, effects of these two parameters are studied for enhanced system performance. An initial assumption is made on the cycle which the produced liquid hydrogen is 1 kmole/s. Thus, the yield of this cycle corresponds to 1 kmole/s and remaining is assumed to be collected first from the Mg-Cl cycle. The cycle shows 11.56% yield at the base case model. Effect of compressor outlet pressure on liquid hydrogen yield and specific work is represented in Fig. 6. Higher outlet pressure is favorable for both yield and specific work of the system. It is expected that higher pressure would result in higher work consumption, however, power consumption of nitrogen liquefaction is also strongly affected by this parameter.

A general efficiency assessment of the precooled liquefaction cycle is made based on the liquid hydrogen yield from the cycle. However, energy and exergy efficiencies are calculated based on main inputs and outputs to and from the system. Since the chemical exergy of hydrogen is very high, its physical exergy content does not influence the system performance as much as its chemical exergy content. However, all values related to physical exergy change of hydrogen are included in the efficiency assessment. The effect of compression pressure on the system performances are also presented in Fig. 7. All performance parameters show a

decreasing trend after 85 bar, due to relatively higher work consumption of the cycle. Thus, compression pressure is set to 85 bar, and heat exchanger effectiveness is kept at 85% in order to keep the cycle performance characteristics at a reasonable rate.

The energy efficiency of the plant for the base case is found to be 42.7%, where the exergy efficiency is 63.7%. The total electrical work requirement to run the cycle including nitrogen liquefaction is found to be 156.46 MW to liquefy 1 kmole/s hydrogen. The total exergy destruction of the system is found to be 144.38 MW where the highest contribution is made by heat exchangers in the system. Compared to hydrogen compression plant, liquefaction cycle shows higher work requirement. However, transportation of compressed hydrogen is costly and higher volume requirement of compressed hydrogen may not be feasible for use in mobile applications.

4.3. Nuclear Rankine cycle subsystem

A reheat and regeneration type steam Rankine cycle (SRC) is considered for enhanced cycle performance, where the nuclear reactor is used as the boiler of the cycle. The total energy input of the nuclear reactor is based on total heat requirements of the Mg-Cl cycle SRC plant. Initially SRC plant is modeled and analyzed based on total power requirement of liquefaction and Mg-Cl cycle

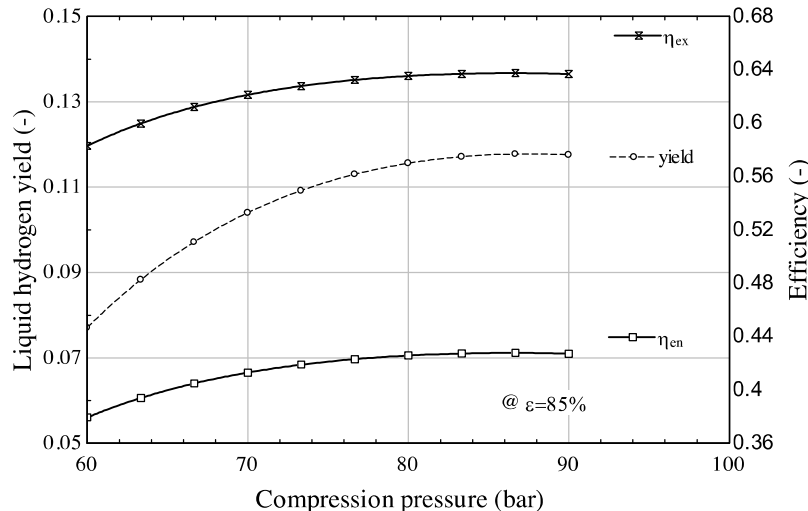


Fig. 7. Effect of compression pressure on efficiencies.

Table 10

State point information for the Steam Rankine cycle subsystem.

State	\dot{m} (kg/s)	T (°C)	P (bar)	h (kJ/kg)	s (kJ/kgK)	ex (kJ/kg)	\dot{Ex} (MW)
17 ^a	354.8	224.1	100	964.3	2.541	211.6	75.061
2	354.8	500	100	3374	6.597	1413	50.1154
3	45.06	341.9	34.18	3086	6.638	1112	50.097
4	309.7	198.7	10	2824	6.687	836.2	25.8985
5	309.7	500	10	3479	7.762	1170	362.348
6	42.7	399.5	5.029	3271	7.789	953.9	46.661
7	267	35.23	0.057	2463	8.017	78.62	20.504
8	267	35.23	0.057	147.6	0.5081	0.645	0.1682
9	267	35.28	5.029	148.2	0.5085	1.149	0.299.8
10	309.7	152.1	5.029	641.3	1.863	90.58	28.055
11	309.7	153.7	100	654.3	1.869	101.7	31.503
12	309.7	221.2	100	951.4	2.515	239.3	74.107
13	45.06	241.2	34.18	1043	2.713	239.3	10.781
14	45.06	243.2	100	1053	2.717	248.2	11.184

^a Mass flow for the Mg–Cl cycle HEX is not included.

which is found to be 453.6 MW. State point information and T-s diagram of the cycle is presented in Table 10 and Fig. 8, respectively. The present cycle shows relatively higher performance results than that of conventional SRC plants with reheating and regeneration. The net power output is set to a constant number which is sum of power requirements of Mg–Cl and liquefaction cycles. The mass flow rate of the system is calculated based on this constant number. The parametric studies are conducted to generally decrease the heat requirement of the cycle by manipulating various system and environmental parameters. The fractions of the turbine leaks (f_1 and f_2) are calculated by writing an energy balance for FWH and regenerator, respectively, where fraction of state 3 and 6 correspond to 12.7% and 15.8%.

The extraction pressures are initially assumed constant numbers with reasonable assumptions, and an optimization is applied to enhance the energy performance of the cycle. Both energy and exergy efficiencies of the SRC system result in 42.9%, and 62.8%, respectively, for the base model. The energy efficiency of the plant is superior to conventional plants. The total heat requirement to run the cycle and produce desired power is found to be 1058 MW.

The effects of boiler pressure on system mass flow rate, exergy efficiency, and plant input and output are represented in Figs. 9 and 10. The higher boiler pressure influences all parameters with a similar trend but the mass flow rate. For the sake of a more compact design, 85–90 bar range can be a feasible selection, even

if it does not show promising performance values. Both heat input and net power output decrease at higher boiler pressures, where decrease in heat input is higher, which leads to a higher exergy efficiency.

The effects of turbine inlet temperature and ambient temperature on exergy performance of the system and mass flow rate are also represented in Fig. 11. A higher turbine inlet temperature at lower ambient temperatures are not favorable for system exergy performance, but it is highly effective on lower mass flow rate within the system. Lower exergy efficiency values are due to higher thermal exergy of the input energy at elevated temperatures. A more compact design of the system can be made by higher turbine inlet temperature and boiler pressure, where it is not much effected by the environmental parameters.

The heat requirement of the MgCl cycle is also compensated by the nuclear reactor by providing 248.58 MW of energy to HEX of the cycle. Grade of the heat is kept higher than 320 °C, and steam is used as the heat transfer fluid. The total heat provided by the nuclear cycle to run the integrated system is found to be 1306.58 MW. The efficiency assessment of the integrated system can now be made by calculating efficiencies based on main inputs and outputs to and from the system. The total energy and exergy efficiencies of the plant are found to be 18.6%, and 31.35%. It should be noted that energy and exergy efficiencies of uranium processing are 33%, and 26.7%, respectively (Ozbilen et al., 2012). However, these

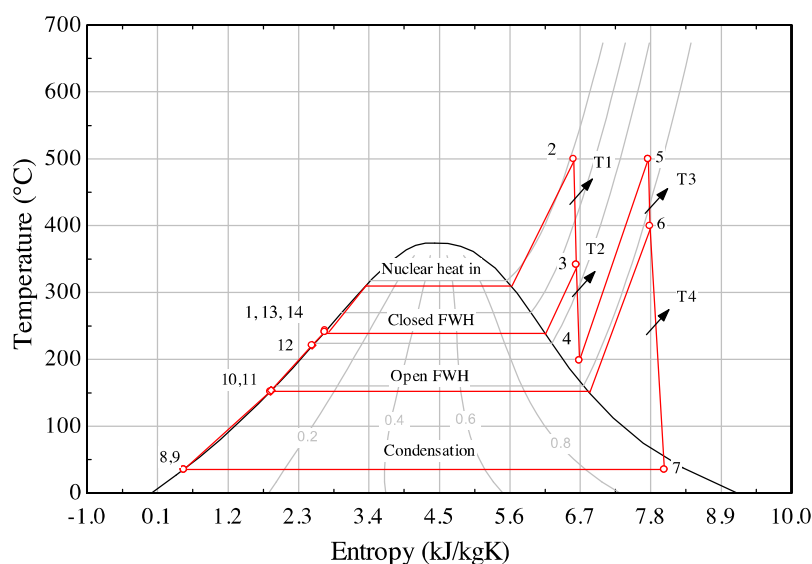


Fig. 8. T-s diagram of the SRC plant.

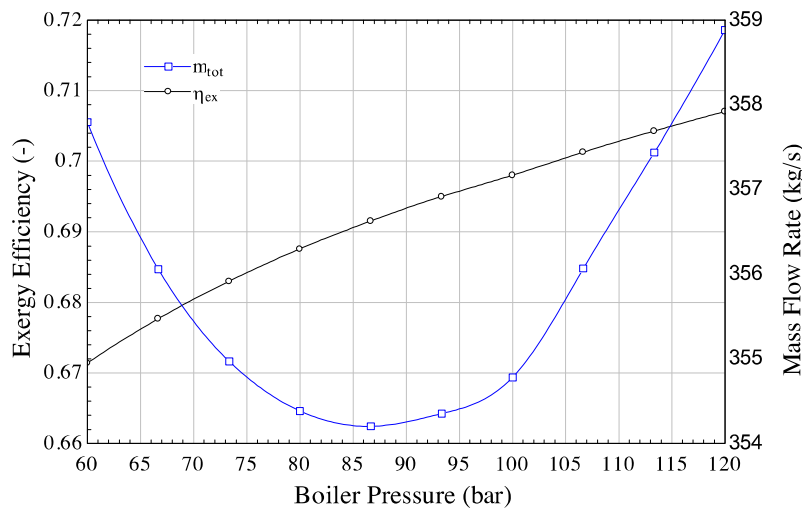


Fig. 9. Effect of boiler pressure on mass flow rate and exergy efficiency of the SRC plant.

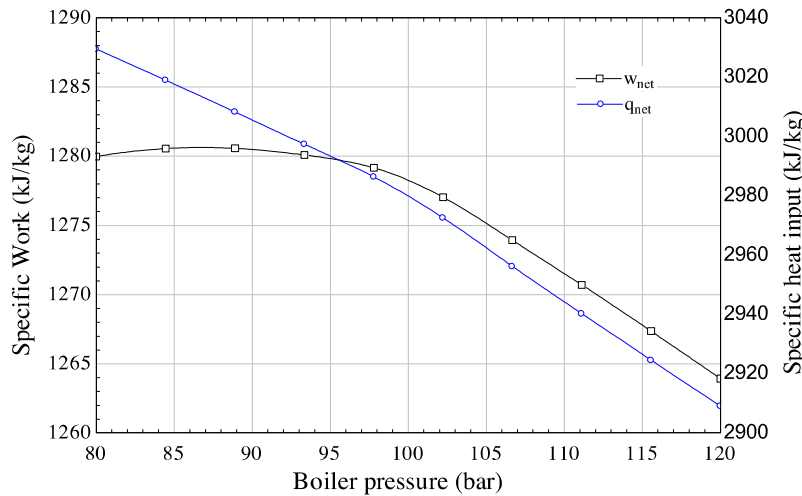


Fig. 10. Effect of boiler pressure on net specific work and heat.

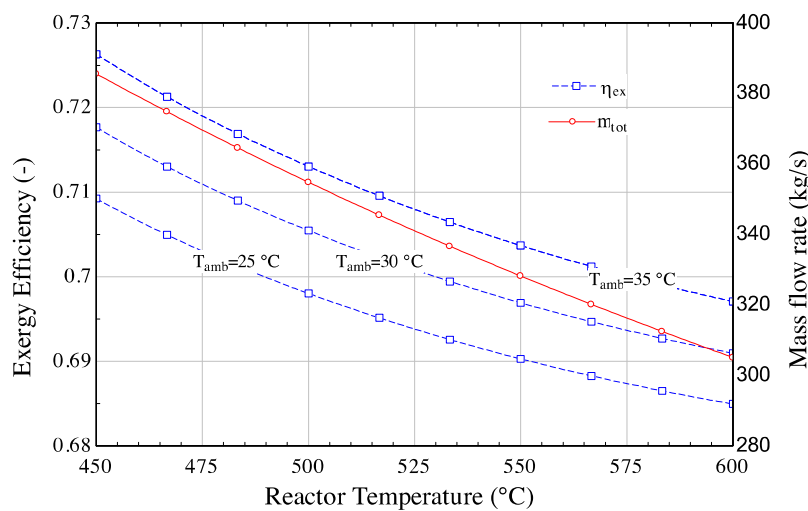


Fig. 11. Effect of turbine inlet temperature and ambient temperature on system exergy performance and mass flow rate.

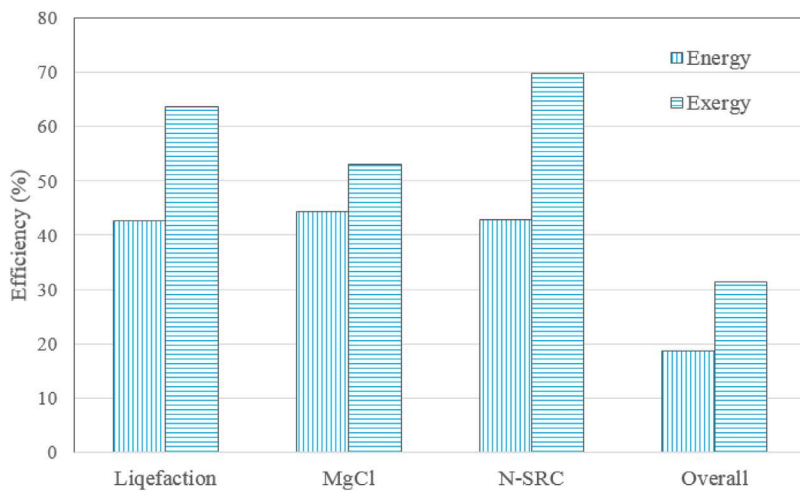


Fig. 12. Efficiency comparisons of subsystems.

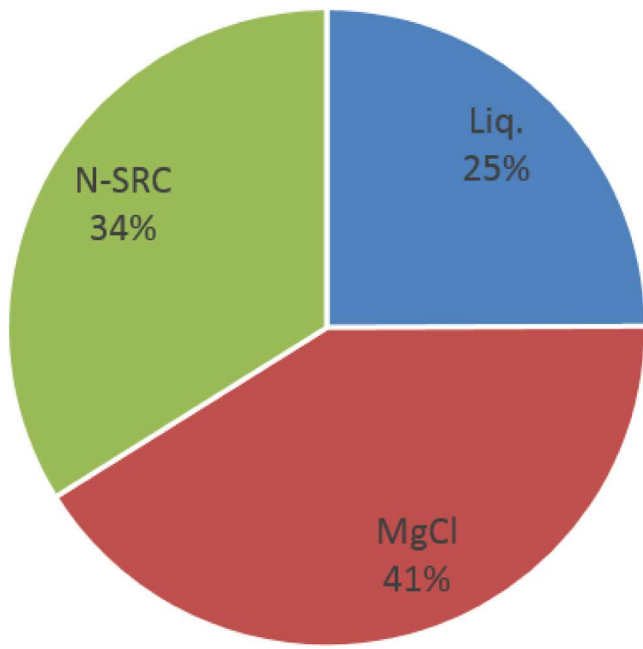


Fig. 13. Exergy destruction ratios of subsystems of System II.

values are not considered for the total performance assessment of the plant. The comparisons of the subsystem efficiencies and total exergy destructions are illustrated in Figs. 12 and 13. Here, highest irreversibility ratio belongs to the Mg Cl cycle by 41%.

5. Conclusions

This study performs a comprehensive thermodynamic analysis for a nuclear based integrated hydrogen production and liquefaction plant. Mature electrolysis technology, reliable chemistry through reactors, relatively low maximum temperatures and acceptable efficiency values makes the four-step Mg Cl cycle a feasible system for hydrogen production. The electrical work consumption of the four-step Mg Cl cycle is also up to %6.7 lower than that of conventional water electrolysis at a specific current density. Although the liquefaction of hydrogen requires large amounts of power, a higher density of the liquid hydrogen makes it a feasible option for a more economic transportation to end users. The

present system is also suitable to be scaled up for off-peak hydrogen generation from nuclear plants.

References

- Aspen plus user guide, 2003. Aspen Technology Limited, Cambridge Massachusetts.
- Bracha, M., Lorenz, A., Patzelt, A., Wanner, M., 1994. Large-scale hydrogen liquefaction in Germany. *Int. J. Hydrot. Energy* 19 (1), 53–59.
- Dincer, I., Kanoglu, M., 2011. *Refrigeration Systems and Applications*. John Wiley & Sons, UK.
- Dincer, I., Rosen, M.A., 2012. *Exergy: Energy, Environment and Sustainable Development*. Newnes, UK.
- Dincer, I., Zamfirescu, C., 2012. Sustainable hydrogen production options and role of AIHE. *Int. J. Hydrot. Energy* 37, 16266–16286.
- Georgis, D., Jogwar, S.S., Almansoori, A.S., Daoutidis, P., 2011. Design and control of energy integrated SOFC systems for in situ hydrogen production and power generation. *Comput. Chem. Eng.* 35 (9), 1691–1704.
- Hesson, R.N., 1979. *Kinetics of the Chlorination of Magnesium Oxide*, M.Sc. Thesis. Ames Lab., IA.
- Kashani-Nejad, S., Ng, K.-W., Harris, R., 2004. Preparation of MgOHCl by controlled dehydration of MgCl₂·6H₂O. *Metall. Mater. Trans. B* 35, 405–406.
- Kashani-Nejad, S., Ng, K.-W., Harris, R., 2005. MgOHCl thermal decomposition kinetics. *Metall. Mater. Trans. B* 36, 153–157.
- Kelley, K.K., 1945. *Energy Requirements and Equilibria in the Dehydration, Hydrolysis, and Decomposition of Magnesium Chloride*, vol. 676. US Govt. Print. Off.
- Klein, S., Nellis, G., 2012. *Thermodynamics*. Cambridge University Press, NY.
- Kotas, T.J., 2013. *The Exergy Method of Thermal Plant Analysis*. Elsevier, UK.
- Montazer-Rahmati, M.M., Binaee, R., 2010. Multi-objective optimization of an industrial hydrogen plant consisting of a CO₂ absorber using DGA and a methanator. *Comput. Chem. Eng.* 34 (11), 1813–1821.
- Nandi, T.K., Sarangi, S., 1993. Performance and optimization of hydrogen liquefaction cycles. *Int. J. Hydrot. Energy* 18 (2), 131–139.
- Naterer, G.F., Dincer, I., Zamfirescu, C., 2013. *Hydrogen Production from Nuclear Energy*. Springer, London.
- Ozbilen, A., Dincer, I., Rosen, M.A., 2012. Exergetic life cycle assessment of a hydrogen production process. *Int. J. Hydrot. Energy* 37 (7), 5665–5675.
- Ozcan, H., Dincer, I., 2014a. Performance investigation of magnesium-chloride hybrid thermochemical cycle for hydrogen production. *Int. J. Hydrot. Energy* 39, 76–85.
- Ozcan, H., Dincer, I., 2014b. Energy and exergy analyses of a solar driven Mg-Cl hybrid thermochemical cycle for co-production of power and hydrogen. *Int. J. Hydrot. Energy* 39, 15330–15341.
- Ozcan, H., Dincer, I., 2015a. Thermodynamic and environmental impact assessment of steam methane reforming and magnesium-chlorine cycle-based multigeneration systems. *Int. J. Energy Res.* 39, 1778–1789.
- Ozcan, H., Dincer, I., 2015b. Comparative performance assessment of three configurations of magnesium-chlorine cycle. *Int. J. Hydrot. Energy* 41, 845–856.
- Ozcan, H., Dincer, I., 2016. Modeling of a new four-step magnesium-chlorine cycle with dry HCl capture for more efficient hydrogen production. *Int. J. Hydrot. Energy* 41, 7792–7801.
- Ozcan, H., 2015. *Experimental and Theoretical Investigations of Magnesium-Chlorine Cycle and Its Integrated Systems*, Phd Thesis. University of Ontario Institute of Technology, 2015.
- Zhu, L., Zhang, Z., Fan, J., Jiang, P., 2016. Polygeneration of hydrogen and power based on coal gasification integrated with a dual chemical looping process: thermodynamic investigation. *Comput. Chem. Eng.* 84, 302–312.